Earthquake Engineering & Structural Dynamics

WILEY

RESEARCH ARTICLE

Seismically Isolated Nuclear Power Plants: Is Soil–Structure-Interaction Analysis Needed?

Kaivalya M. Lal[1] | Andrew S. Whittaker[2] | Shahriar Vahdani[3] | Benjamin D. Kosbab[4] | Koroush Shirvan[5]

[1]Engineer, Structural Integrity Associates, Inc., Atlanta, Georgia, USA, formerly, Ph.D. student, University at Buffalo, The State University of New York, Amherst, New York, USA | [2]SUNY Distinguished Professor, University at Buffalo, The State University of New York, Amherst, New York, USA | [3]President, Applied Geodynamics Inc., El Cerrito, California, USA | [4]Senior Principal, Simpson Gumpertz & Heger, Atlanta, Georgia, USA | [5]Professor, Massachusetts Institute of Technology, Cambridge, Massachusetts, USA

Correspondence: Kaivalya M. Lal (klal@structint.com)

Received: 1 December 2024 | **Revised:** 7 April 2025 | **Accepted:** 2 May 2025

Funding: This study was funded by the U.S. Department of Energy under its Advanced Reactor Concept (ARC-20) project, Award Number DE-NE0009049.

Keywords: nuclear reactor buildings | seismic isolation | soil–structure interaction | surface free-field motions

ABSTRACT

This study assesses the need for soil–structure interaction (SSI) analysis of surface- or near-surface mounted, seismically isolated nuclear power plants (NPPs). The current rules and guidance for SSI analysis of NPPs are based on the legacy assumption that reactor buildings are stiff and heavy: the two key attributes needed for significant SSI on soil sites. Reactor developers in the United States are considering seismic isolation as a design feature to reduce the impact of the seismic load case and to enable standardization. The substantial reduction in lateral stiffness associated with the introduction of horizontally flexible isolators at the base of a reactor building led to the hypothesis that SSI has no meaningful effect on seismic acceleration and displacement demands on structural components and equipment in surface- or near-surface-founded, base-isolated NPPs. Herein, reactor buildings and their safety-class equipment, the supporting soil domains, and nonlinear isolation systems are explicitly modeled and analyzed to judge whether the hypothesis is correct. An extensive set of response-history analyses was performed for 945 combinations of (1) three fundamentally different, surface mounted reactor buildings, (2) five horizontal isolation systems with a range of linear and bilinear properties, (3) nine seismic inputs covering a range of frequencies and amplitudes of shaking, and (4) seven generic soil profiles that cover a range of sites across the United States and were a part of the Design Certification Documents that enabled the KEPCO APR1400 to be certified for use by the United States Nuclear Regulatory Commission under the 10CFR Part 52 licensing framework. The peak resultant horizontal displacements of the isolation systems, peak resultant horizontal accelerations in each reactor building, and in-structure horizontal and vertical acceleration response spectra were essentially identical with and without considerations of SSI, confirming the hypothesis.

1 | Introduction

Two critical barriers to the rapid deployment of new build nuclear power plants (NPPs) are high capital cost and long deployment time (i.e., site selection, analysis, design, licensing, and construction). A key contributor to the high cost and long deployment time is the seismic load case, which is different at each NPP site and requires site-specific activities including geotechnical investigations, probabilistic seismic hazard analysis (PSHA), and soil–structure interaction (SSI) analysis, which are time consuming and expensive.

This study focuses on SSI analysis of surface- or near-surface-founded, horizontally isolated NPPs[1]. The current rules and

regulations for analysis, design, and licensing of NPPs are based on legacy procedures developed decades ago for gigawatt-scale large light water reactors (LLWRs), which are typically very heavy (weighing millions of kN) and stiff (having fundamental frequencies higher than 5 Hz): the two key ingredients for significant SSI on soil sites. Unless constructed on a hard rock site, United States standards and federal regulations (e.g., Section IV.(a).1.(iv) of appendix S to 10CFR50) effectively obligate SSI analysis for the design of an NPP, with the expectation that the soil flexibility *may* substantially change the seismic demands (i.e., in-structure acceleration response spectra) on the safety-related equipment in the reactor building. This requirement is unique to the nuclear industry because SSI analysis is not mandated for non-nuclear, mission-critical buildings in the United States, in part because the expectation is that SSI will reduce accelerations and drifts.

Reactor developers are considering the use of seismic isolation, which introduces 2D or 3D flexibility at the base of a reactor building, to reduce seismic demands on safety-class equipment and enable standardization [1]. The substantial reduction in stiffness of an isolated reactor building, with respect to its conventionally founded counterpart, raises the question "Is SSI analysis needed to compute seismic acceleration and displacement demands on structural components and equipment in surface- or near-surface-founded, base-isolated nuclear reactor buildings?" If not needed, one time-consuming, expensive task of uncertain complexity, which could challenge and delay analysis, design, and regulatory review, and slow NPP deployment, would be eliminated. Instead, surface-free-field representations of ground shaking, derived from PSHA, could be directly used for analysis and design. This paper answers the question in a first-of-a-kind study by modeling and analyzing reactor buildings and their safety-class equipment, isolation systems, and supporting soil domains for a wide range of seismic inputs.

The methods used for PSHA, site-response analysis (SRA), and SSI analysis are not critiqued here because they are not relevant to the hypothesis of this study. Rather, practices and computer codes common in the United States industry, including the nuclear energy sector, are assumed sufficient for the study. Bolisetti and Whittaker [2] provide a comprehensive review of the literature on site-response and SSI analysis before 2015. Lal et al. [3] summarize the literature published since 2015.

2 | Prior Studies on SSI Analysis of Seismically Isolated Structures

Base isolation reduces seismic demands in structures, systems, and components (SSCs) by introducing flexibility and energy dissipation. A very flexible soil domain beneath a base-isolated structure will alter the dynamic properties of the isolated building by increasing the overall flexibility of the soil-structure system and introducing additional energy dissipation through hysteretic and radiation damping in the soil. Research characterizing the impact of SSI on seismically isolated nuclear structures is limited. The SSI studies relevant to the goal of this study are briefly summarized next. More information is presented in Section 1.4 of Lal et al. [3].

Constantinou and Kneifati [4, 5] analytically examined the response of a single-story linear structure isolated using elastomeric bearings modeled as linear viscous elements and supported on a homogeneous, viscoelastic half-space representing the supporting soil. The study considered a range of properties for the structure, isolation system, and supporting soil. Analyses were conducted using harmonic excitations and the 1940 El Centro earthquake record. They concluded that if the ratio of the fundamental frequency of the non-isolated structure (on a rigid support, no soil), f_0, to the fundamental frequency of the isolated structure (also on a rigid support), f_b, is greater than 15, the influence of SSI on the structure and isolation system response is minimal. For values of f_0/f_b less than 15, the principal effect of SSI is to reduce the fundamental frequency of the soil-structure system (i.e., isolated structure with the supporting soil), f_1. If this reduction is less than 5% (i.e., f_1/f_b is greater than 0.95), the influence of SSI is negligible. Constantinou and Kneifati [6] executed a similar study for bilinear isolation systems and observed that SSI effects (1) become less prominent with a decrease in μ (ratio of yield force of the bearings to the weight of the structure) of the bilinear systems and (2) were generally lower for bilinear isolations systems than for linear systems.

Drosos and Sitar [7] analyzed a 3D model of the APR1400 NPP building, modified by the authors from the original design by the Korea Electric Power Corporation (KEPCO) to include a base isolation system. The reactor building was isolated using 454 lead-rubber bearings (LRBs) with an effective period of 2 seconds. Nine soil profiles from the Design Certification Documents (DCDs) of APR1400 were considered. (Information on these soil profiles is presented in Section 5.3). Twenty ground motion triplets were selected and scaled such that their average response spectrum matched the RG 1.60 [8] target spectrum anchored to a peak ground acceleration (PGA) of 0.5 g. The ground motions were applied at the surface free field of each soil profile. The computer program SASSI [9] was utilized to perform a frequency-domain, linear analysis of the combined soil-structure model. The soil profiles were modeled using strain-compatible properties. To establish a baseline, the study included analysis of (1) the isolated reactor building supported on a rigid base (i.e., no soil domain, ignoring SSI effects), and (2) the non-isolated reactor building supported on a rigid base. Results showed that soil compliance had minimal effect on the in-structure response spectra of the isolated reactor building. The acceleration response of the reactor building supported on nine soil profiles (considering SSI effects) was virtually indistinguishable from that of the isolated reactor building supported on a rigid base (without SSI effects): see Figure 6 in that study.

Zhou and Wei [10] analyzed the base-isolated APR1400 model using SASSI, but with soil profiles, ground motions, and an isolation system different than those in Drosos and Sitar [7]. A 180 m deep generic soil profile was used. The shear modulus of the soil profiles was both halved and doubled to investigate the effect of soil stiffness. The isolation system had 219 LRBs and an effective period of 2 seconds. Unidirectional analysis was performed for two horizontal ground motions (one synthetic, GM1, and one earthquake record, GM2) and one vertical motion (=2/3 of GM1). Similar to the approach of Drosos and Sitar [7], the soil profiles

were modeled using strain-compatible properties, and the ground motions were applied at the surface free field for SSI analysis. It was observed that the horizontal spectral accelerations at the top of the RCB with and without considering SSI effects (i.e., isolated building on a rigid support) were virtually identical, with small differences near the fundamental frequencies of the reactor building. The horizontal response on the basemat of the isolated building was unaffected by soil stiffness, implying that the isolation-system behavior was not influenced by soil stiffness. In the vertical direction, the response along the height of the RCB was substantially smaller when SSI effects were included, which was attributed to the damping introduced by the soil.

3 | Standard of Practice for SSI Analysis of Nuclear Structure in the United States

The need for SSI analysis of safety-related nuclear facilities in the United States is addressed in ASCE/SEI Standard 4–16 [11] for DOE-regulated facilities and in NUREG-0800, Standard Review Plan [12] for NRC-regulated facilities, both developed for conventionally founded (i.e., non-isolated) LLWRs.

Section 5.1.1 of ASCE/SEI Standard 4–16 permits analysis assuming a fixed base (i.e., no soil domain, ignoring SSI) if one of the following apply (1) the dominant frequency of the fixed-base facility is less than half the value calculated assuming the facility to be rigid and supported on springs[2] representing the soil domain (also included in ASCE 4–98), (2) the facility is supported on rock with a shear wave velocity exceeding 1,067 m/s (3,500 ft/s), and the analyst can demonstrate that SSI effects are negligible, and (3) the facility is founded on rock with a shear wave velocity greater than 2,400 m/s (8,000 ft/s). Condition 1 is seldom met for conventionally founded nuclear facilities due to their high stiffness, associated with a building envelope constructed of thick reinforced concrete (RC) walls designed, in part, to confine or contain radionuclides, with fundamental horizontal frequencies higher than 5 Hz. Condition 2 necessitates SSI analysis to establish that it is not needed. Condition 3 is applicable only to facilities built on very hard rock, largely limited to a few sites in the Central and Eastern United States.

4 | Analysis Methodology

To assess the significance of SSI on base-isolated NPPs, dynamic analysis is performed for the three cases illustrated in Figure 1:

Case 1	Analysis of a coupled soil-structure system (i.e., an isolated reactor building and the supporting soil domain) following standard United States practice, to include the effects of SSI, if any.
Case 2	Site-response analysis to capture surface free-field motions using the same inputs as those applied to Case 1, to capture the amplification or deamplification of ground motions from the base of a soil profile to the ground surface in the absence of a structure.
Case 3	Analysis of the isolated reactor building using the surface free-field motions from Case 2, without the supporting soil domains, not considering SSI.

If the displacement and acceleration responses of a reactor building and its equipment for Case 1 (denoted as R1 in Figure 1) are *similar* or less than those in Case 3 (R2), SSI is either insignificant from an engineering perspective or beneficial.

There is no industry-wide consensus on the definition of *similar*, in part because the *true* solution will never be known.

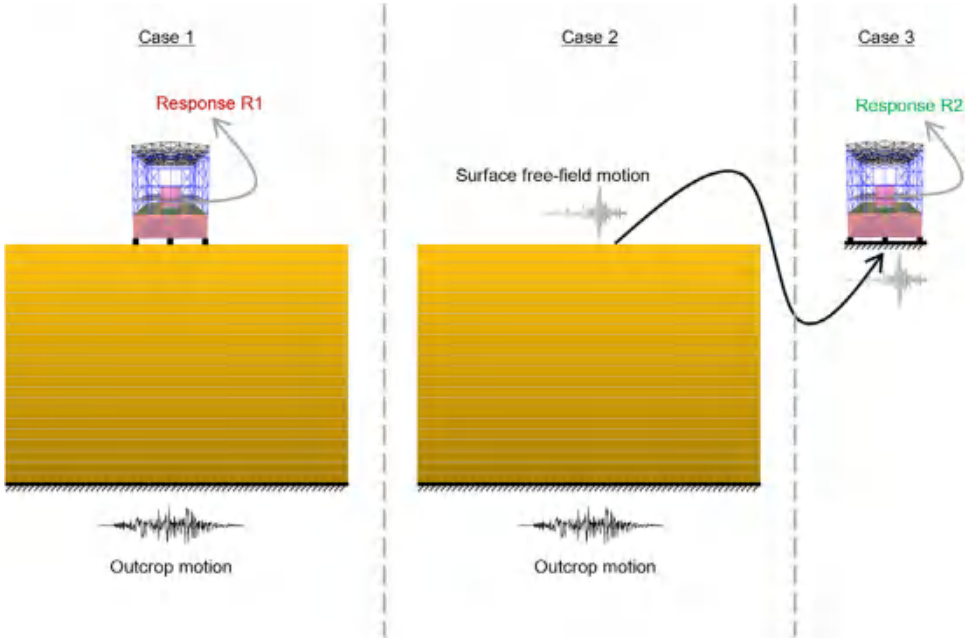

FIGURE 1 | Analysis cases to investigate the effects of SSI on seismically isolated reactor buildings.

Engineering judgment is needed to define *similar*, and the definition, in terms of bounds, should recognize and characterize all the sources of variability and uncertainty included in the calculations. Herein, responses are deemed *similar* if they fall within 15% of the baseline Case 1, noting that the uncertainties and variabilities inherent in SSI analysis, namely, (1) identifying a horizontal soil/rock horizon at depth, from which earthquake shaking is propagated upwards, (2) characterizing ground motion at the level of the horizon, (3) simplification of the heterogenous soil domain into a horizontally layered stratigraphy, (4) the assumption that body waves propagate vertically through the soil domain from the rock horizon, ignoring surface waves (which may dominate hazard for many NPP sites) and inclined body waves, and (5) the idealization of soil domain boundaries, which seeks to represent an *infinite* medium within a finite model, likely warrant a much greater percentage. As a point of reference, Doulgerakis et al. [13], in a report that addressed the validation of finite element programs for SSI analysis using the Lotung experiment data set, used ±25% as a threshold for acceptance. Another point of reference is ASCE/SEI 4–16, wherein ±10% is used in multiple Sections (e.g., 3.1.2.1, 3.1.4, 3.3.1, and C5.1.11) to define sufficiency. The bound of 15% lies between that of ASCE/SEI 4–16 and Doulgerakis et al. [13]. (As presented later in this study, a threshold of 15% is not challenged).

Another dimension to the definition of *similar* is the magnitude of the difference in the responses of interest. For example, the percentage difference between accelerations of 0.05 g and 0.04 g, and between 1.00 g and 0.80 g, is 20, but the difference in magnitude differs by more than an order of magnitude. In the former case, the 20% difference (0.05–0.04 g) is of no engineering significance. In the latter case, the 20% difference of 0.20 g may be important. Both dimensions to *similar* are considered herein, with emphasis placed first on the percentage difference.

Finite element programs such as ABAQUS [14] and LS-DYNA [15] are used for direct SSI analysis in the United States nuclear industry. Herein, the commercial finite element program SAP2000 [16] is used because it employs a widely used, computationally efficient algorithm, namely, Fast Nonlinear Analysis (FNA), which is well suited for time-domain analysis involving nonlinear elements (such as nonlinear seismic isolators) and is orders of magnitude faster than other commercial codes solving similar problems[3].

The requirements for employing FNA are that a numerical model must have a limited number of nonlinear members and that the nonlinear behavior must be confined to link elements. This is possible for the SSI analysis in this study since (a) the response of a base-isolated superstructure is expected to be (and modeled as) linear elastic, (b) the nonlinear response of the APR1400 soil profiles is captured indirectly using the equivalent-linear approach as described in Section 6, and (c) the only nonlinear elements, the seismic isolators and dampers, are modeled using United States industry-practice link elements, enabling the use of FNA. Using this approach, SSI analysis of a base-isolated reactor building, with run times of tens of hours in LS-DYNA or ABAQUS, can be completed in a few minutes using FNA in SAP2000, enabling the 1000+ simulations performed in this study.

5 | Analysis Matrix

Response-history analysis is performed for combinations of reactor buildings, isolation systems, soil profiles, and seismic inputs summarized next and in Figure 2. More information is presented in Section 2 of Lal et al. [3].

5.1 | Reactor Buildings and Foundation

Three advanced reactor buildings (Figure 2a) are considered in this study to ensure that the outcomes were broadly applicable. The geometry and layout of the buildings and their sample equipment are fundamentally different, in addition to the reactor technology.

Horizontal-compact high temperature gas reactor (HC-HTGR): A numerical model of an early version of the Boston Atomics HC-HTGR building was developed by Parsi et al. [17]. It is a 10 m tall, RC structure with plan dimensions of 14 m × 75 m. The building includes six major compartments: entry (red in Figure 2a), reactor maintenance (green), control operations (yellow), primary system (gray), fuel storage (purple), and refueling (orange). The entry, control operations, and fuel storage compartments are multistory; all others are single story. The building has a 1.2-m-thick perimeter RC wall adjacent to the primary system compartment, sized for radiation shielding. The remaining perimeter walls are 0.75 m thick. The floor slabs and partition walls between the compartments are 0.45 m thick. The basemat is 1.2 m thick. The primary system is aligned horizontally and integrates the reactor vessel (RV), steam generator (SG), and helium circulator. The building and its equipment weigh 117,000 kN. Modal analysis is performed to identify the dominant frequencies of the fixed-based reactor building and the primary system. In the H1 and H2 directions (see Figure 2a for the coordinate system), the dominant frequencies of the reactor building (primary system) are at 27.3 Hz (4 Hz) and 14.4 Hz (5 Hz), respectively. In the vertical direction, the mass of the building and the primary system is distributed across several modes with frequencies between 20 and 50 Hz.

Fluoride salt-cooled high temperature reactor (FHR): Mir et al. [18] developed a numerical model of an early version of the Kairos Power FHR building. It has plan dimensions of 25 m × 25 m and the height from the basemat to the peak of the roof is 33 m. The building includes four floors: an RC basemat, a suspended RC floor (green), and two composite floors (yellow). At the center of the building is a cylindrical RC shield structure (pink) with a diameter of 8.8 m, which extends from the basemat to an elevation of 18 m. The basemat and the suspended floor are 1.2 m thick. The composite floors consist of a 76 mm concrete slab atop a 76 mm deep metal deck, modeled as a concrete slab with an equivalent thickness of 114 mm. Above the suspended RC floor, the building is non-safety class and is framed in structural steel designed to commercial building standards. The part of the building below the suspended RC floor is assumed to be safety-related and houses one RV, one RV auxiliary cooling system (RVACS), and four primary heat exchangers. The RV and RVACS are located inside the central shield structure. The total weight of the FHR building, including its equipment, is 87,000 kN. The dominant frequencies of the fixed-based building and its equipment in the

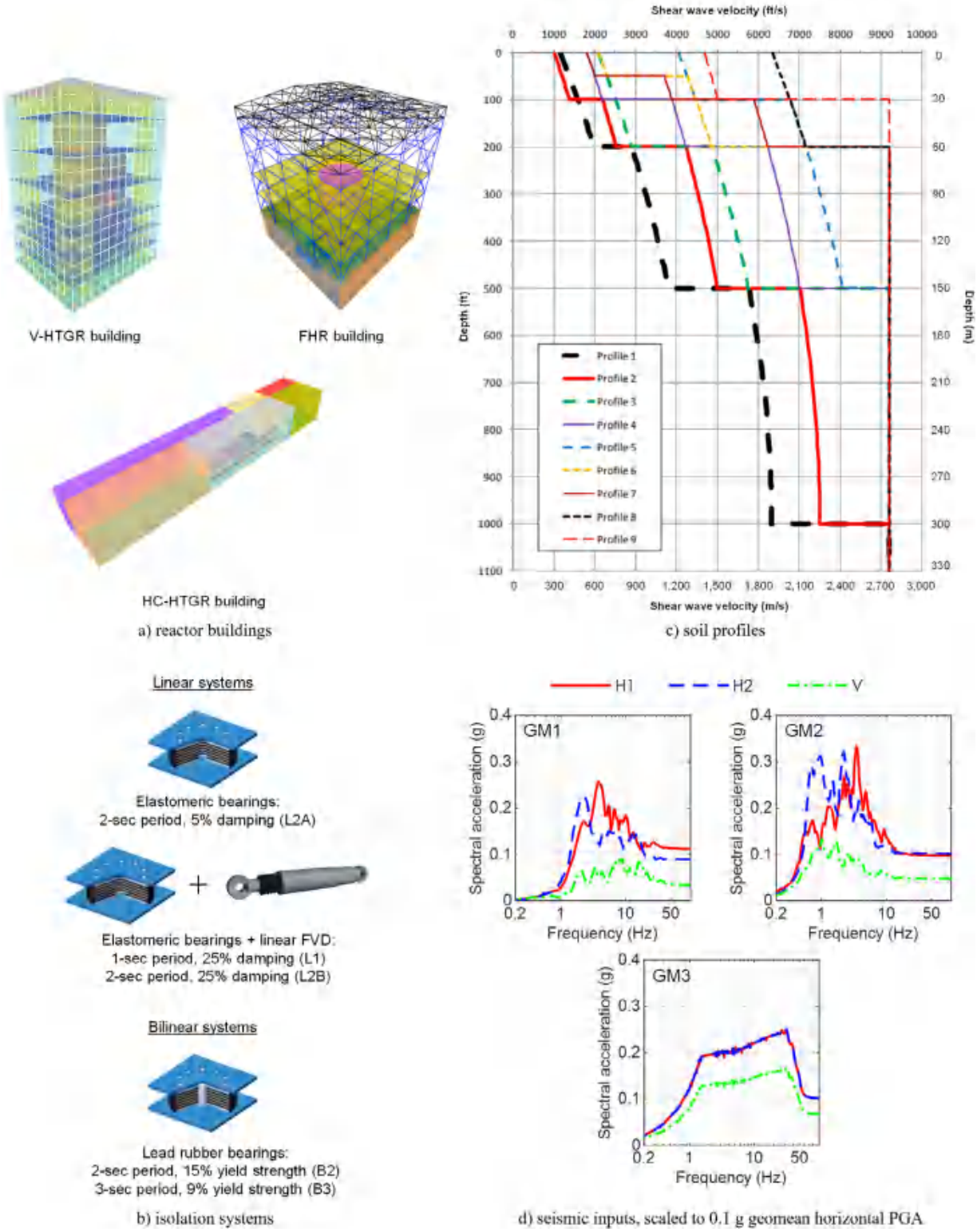

FIGURE 2 | Analysis matrix.

two horizontal (vertical) directions are: 10 Hz (24 Hz) for the reactor building, 13 Hz (37 Hz) for the RV, and 7 Hz (27 Hz) for the RVACS.

Vertically configured high temperature gas reactor (V-HTGR): Parsi et al. [1] developed a numerical model of an early version of X-energy's Xe-100: a high temperature gas reactor. It is a multistory RC structure with plan dimensions of 24 m × 20 m and a height of 34 m. The perimeter walls, which support the floor slabs, are 0.45 m thick. The building has two RC citadels, one housing the RV and extending from the basemat to the roof, and the other housing the SG and extending 24 m up from the basemat. The RV and SG are supported on the fourth floor of the building, 12 m above the basemat. The weight of the building and its equipment is

113,000 kN. The dominant frequencies of the fixed-based building and its equipment in the two horizontal directions are: 5–6 Hz for the reactor building, 8 Hz for the RV, and 13 Hz for the SG. The mass of the building and equipment is distributed across several modes in the vertical direction, for which well-defined frequencies could not be identified.

For each reactor building, the foundation mat extends three meters beyond the exterior envelope in both the horizontal directions and has a depth of 1.8 m, with the foundations embedded in the soil domains to this full depth (i.e., the top of foundation is at grade). The 3-m extension of the foundation mat accommodates the unrestricted movement of the base-isolated superstructure and provide a foundation for perimeter below-grade construction such as a retaining wall. The conclusions of this study are not sensitive to the projection of the foundation beyond the building envelope.

5.2 | Isolation Systems

Five isolation systems (Figure 2b) are considered in this study, all of which use isolators and dampers that are commercially available in the United States and have seen widespread use in non-nuclear sectors for more than three decades. Of the five, three are linear and two are bilinear. All five systems are 2D and isolate in the horizontal plane only. The isolation systems span a wide range of periods and damping to ensure that recommendations of this study are broadly applicable to all plausible isolation systems. None of the isolation systems are optimized for the location of isolators, weight of the reactor buildings, intensity and frequency content of the seismic hazard, and properties of underlying soil domain. Generic isolation system properties are considered. The isolation systems have a total of 48, 17, and 30 isolators for the HC-HTGR, FHR, and V-HTGR buildings, respectively.

Three linear systems with a 1-second period and 25% damping (L1); a 2-second period and 5% damping (L2A); and a 2-second period and 25% damping (L2B) are analyzed. Systems L1 and L2B are composed of low-damping natural rubber (elastomeric) bearings with supplemental uniaxial fluid viscous dampers (FVDs). System L2A is composed of only low-damping natural rubber bearings. Twenty-five percent damping is considered for L1 and L2B to judge the effect, if any, of high levels of damping in the isolation system on the hypothesis that SSI analysis is not needed for base-isolated NPPs. Information on low-damping natural rubber bearings and FVDs can be found in Kumar et al. [19] and Makris and Constantinou [20], respectively.

Two bilinear lead-rubber (LR) bearing systems are analyzed, one with a 2-second isolation period and lead cores with a collective yield strength of 15% of the building's gravity weight (B2), and the other with a 3-second period and lead cores with a collective yield strength of 9% of the building's gravity weight (B3)[4,5]. Information on LR bearings is available in Kelly et al. [21], Constantinou et al. [22], and Kumar et al. [19].

Since the isolation systems are not optimized, their vertical stiffness is set to achieve a vertical frequency of 25 Hz, assuming the superstructure to be rigid. A damping ratio of 5% is assigned in the vertical direction.

5.3 | Soil Profiles

Seven soil profiles, S1 through S6 and S9 (profiles 1 through 6 and 9 in Figure 2c), extracted from the DCDs of the APR1400 pressurized water reactor, are used for dynamic analysis. These soil profiles were developed by KEPCO to enable site independent SSI analysis and design of SSCs in APR1400. The $V_{s,30}$ for these profiles range between 300 m/s (defined as the minimum shear wave velocity for competent material supporting the foundation for a [new] NPP per Section 3.7.2 of NUREG-0800, *Standard Review Plan*) and 2,000 m/s, and the depth to the bedrock (taken as the horizon with a shear wave velocity of 2,800 m/s) ranges between 30 and 300 m. (For reference, the site classes per Section 20.2 of ASCE/SEI 7–22 [23] for soil profiles S1 through S6 and S9 are: S1 = CD, S2 = CD, S3 = BC, S4 = C, S5 = B, S6 = B, and S9 = B.) The low-strain (i.e., shear modulus at zero shear strain, G_0) fundamental frequencies (site periods) for these soil profiles are between 1.5 Hz (0.67 seconds) and 12.5 Hz (0.08 seconds), with the higher frequencies corresponding to the soil profiles with greater shear wave velocities. These profiles, from soft soil to hard rock, represent a very wide range of site conditions for possible NPP deployments in the United States and enabled explicit considerations of lower and upper bound soil properties for each profile to be set aside in this study. Analysis was not performed for profiles S7 and S8 because their low-strain fundamental frequencies of 6.7 Hz and 8.8 Hz, respectively, are bounded by those for S6 (= 5.6 Hz) and S9 (= 12.5 Hz).

5.4 | Seismic Inputs

Three ground motion triplets (Figure 2d) are utilized, two from the PEER NGA ground motion database (GM1, GM2) and one synthetic broadband motion (BBM, GM3), collectively covering a very broad range of frequencies (0.3 Hz to 50 Hz) in the horizontal and vertical directions. The earthquake motions were chosen such that one triplet has significant frequency content in the horizontal direction in the *low* range, between 0.3 Hz and 15 Hz (RSN 789), and the other triplet has significant frequency content in a *higher* range, between 1 Hz and 30 Hz (RSN 4083), encompassing the horizontal fundamental frequencies of the soil profiles (1 Hz to 12 Hz), reactor buildings and their equipment (1 Hz to 30 Hz), and isolation systems (0.3 Hz to 1 Hz) considered in this study. Both earthquake triplets were recorded on rock and so provide appropriate inputs at a rock horizon for SSI analysis. The synthetic BBM was developed by Mir et al. [24] by matching a seed motion to a target broadband spectrum, with significant frequency content between 1 and 50 Hz, using RSPMatch2005 [25]. Both the horizontal components were matched to the same broadband spectrum and the ordinates of the spectrum of the vertical component are two-thirds of the (geomean) horizontal spectrum. The BBM is assumed to be a rock motion.

The three ground motion triplets are amplitude scaled to different intensities of shaking at the rock horizon, described in terms of geomean horizontal PGA of (A) 0.1 g: the minimum level of ground shaking often considered for design of United States NPPs, (B) 0.3 g: a typical level of ground shaking used for standard design certification of United States NPPs, albeit at the foundation level and not the rock horizon, and (C) 0.5 g: 1.67 times 0.3 g; considered for risk calculations in support of some design

certifications. The resulting ground motions are GM1A, GM1B, GM1C, GM2A, GM2B, GM2C, GM3A, GM3B, and GM3C.

The surface free-field peak horizontal accelerations will not equal the peak values at the rock horizon, with differences driven by the intensity of the input and nonlinear site response. The lack of constant values of peak geomean horizontal acceleration at the surface free-field is not a shortcoming because the goal here is to characterize the importance of SSI and not to design a reactor building and its equipment.

In summary, a total of 1,890 response-history analyses are performed, 945 for Case 1 in Figure 1, considering SSI, and 945 for Case 3, to derive in-structure responses without the inclusion of SSI. This robust dataset is used to assess the impact of SSI on seismically isolated reactor buildings, after down selection as noted in Section 8.2.2.

6 | Numerical Modeling

Numerical modeling of the reactor buildings and their equipment, foundations, isolation systems, and soil profiles is summarized below. Detailed information is presented in Sections 3 and 4 of Lal et al. [3].

The reactor building perimeter walls, floor slabs, basemat, and the safety-class equipment are modeled using elastic shell elements. The steel framing and RVACS in the FHR building are modeled using elastic beam elements. The foundations are modeled using eight-node elastic solid elements. The interface between the foundation and surrounding soil layers is modeled using common nodes to enforce full connectivity. (Since a seismically isolated advanced reactor building will transmit significantly smaller forces to the supporting soil domain compared to a conventionally founded reactor building, it is assumed that no sliding or gaping would occur at the foundation-soil interface.) Damping in the reactor buildings and the equipment is set to 4% and 2% of critical, respectively, per ASCE/SEI 4–16, and is assigned in SAP2000 using the *material damping* option. The linear and bilinear isolation systems are modeled using the *Linear Spring* and *Rubber Isolator* link element, respectively, in SAP2000. Per Sarlis and Constantinou [26], near-zero modal damping is assigned for the purely isolated modes for response-history analysis of isolated structures using FNA.

The soil profiles are discretized into a significant number of horizontal layers and modeled using eight-node elastic solid elements. The maximum thickness of the soil layers is determined iteratively to achieve a target wave passage frequency (between 15 Hz and 50 Hz, depending on the degraded shear wave velocity of a soil profile) for the vertically propagating body waves (see appendix B in Lal et al. [3]). Orthotropic material properties are assigned to the solid elements, which enables the definition of different values for stiffness in the three principal directions (H1, H2, and V). The horizontal stiffness is defined using two shear moduli, one each for H1 and H2, and the vertical stiffness is characterized by the elastic modulus. Nonlinearity in the soil domains, that is, the reduction in shear modulus and increase in damping as a function of increasing shear strain in the soil layers during earthquake shaking, is captured indirectly via a two-step process. First, a frequency-domain, equivalent linear SRA is performed in DEEPSOIL [27], a widely used SRA tool in the United States commercial sector and nuclear industry, to derive strain-compatible values of shear modulus and damping[6], consistent with the strain demand in each layer, for each of the seven soil profiles and nine seismic inputs. Second, these strain-compatible properties are utilized to generate linear soil models in SAP2000. Because DEEPSOIL only performs 1D SRA, the strain-compatible shear modulus for each layer is computed separately in the H1 and H2 directions for input to SAP2000. Damping in the soil layers is defined using the *material damping* option. Unlike stiffness, damping cannot be assigned different values in the three principal directions in SAP2000, and so is assigned a value equal to the average of the values in H1 and H2, by soil layer, determined in the DEEPSOIL analysis.

The vertical stiffness of the soil columns is assumed not to degrade with ground shaking, and elastic moduli corresponding to low-strain properties are assigned to the soil layers in the vertical direction, consistent with industry practice. To avoid amplification or deamplification of the vertical motion through the equivalent-linear soil columns, the vertical inputs for the SSI analysis were generated by deconvolving the V-direction time series of the scaled triplets to the base of the soil profile[7].

The plan dimensions of the soil domains are selected iteratively such that waves propagating away from the isolated reactor buildings dissipate before reaching the lateral boundaries to avoid reflections. Equal displacement constraints are applied to the lateral boundaries of the soil domains to enforce equilibrium conditions. The plan dimension of the soil domain for the HC-HTGR, V-HTGR, and FHR building is determined to be 370 m × 230 m, 140 m × 140 m, and 152 m × 152 m, respectively.

The soil-rock interface at the base of the soil domains in horizontal directions is modeled as a transmitting boundary in the form of Lysmer dampers [28] using the *Exponential Damper* link element in SAP2000 to radiate outgoing waves. Horizontal ground motion is input as a shear stress history at the base of the soil profile. Since the deconvolved vertical inputs were derived as *within* motions[8], a rigid boundary is modeled in the vertical direction, and the vertical ground motions are applied as acceleration time series. Figure 3 presents the SSI analysis model of the V-HTGR building in SAP2000 for soil profile S1.

7 | Benchmarking of SAP2000

Although widely used by the structural engineering industry in the United States and abroad, SAP2000 has not been used to-date for SSI analysis of NPPs to the knowledge of the authors. Accordingly, it is important to benchmark SAP2000 against other finite element codes and available experimental data. To that end, SAP2000 is benchmarked for site-response and SSI analysis.

7.1 | Site-Response Analysis

Surface free-field response of the APR1400 soil profiles obtained from SAP2000 is compared with that from DEEPSOIL. This comparison serves to confirm the propagation of earthquake

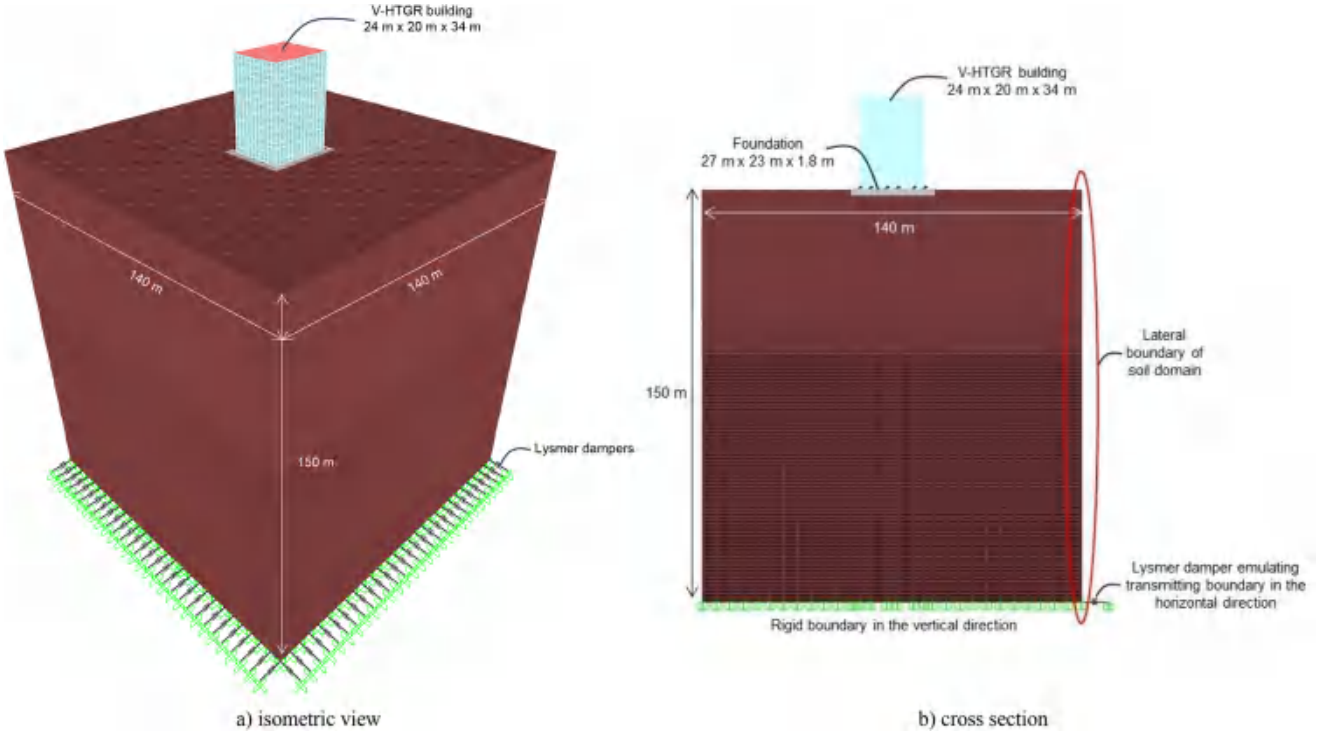

FIGURE 3 | SSI analysis model for the V-HTGR building in SAP2000 for soil profile S1.

waves through a soil profile in SAP2000. Site-response analysis is performed in DEEPSOIL and SAP2000 for the seven APR1400 soil profiles and the nine seismic inputs described in Section 5. Because DEEPSOIL allows only 1D SRA, results are derived separately for the two horizontal components of a seismic input. For SRA in SAP2000, all three components of seismic inputs are applied simultaneously.

Surface free-field acceleration histories are extracted from both computer programs and are used to generate 5%-damped acceleration response spectra. Figures 4 and 5 present the free-field acceleration spectra for soil profile S1, seismic input GM1C and soil profile S2, seismic input GM2A, respectively. A complete set of results is presented in Section 3.2.5 of Lal et al. [3]. In the horizontal directions, the results of linear SRA in SAP2000 using strain-compatible soil properties are in excellent agreement with the equivalent-linear, frequency domain analysis results from DEEPSOIL. In the vertical direction, the free-field spectra match those of the input motions. The small differences in the SAP2000 and DEEPSOIL spectra are attributed to the implementation of damping in the two codes: an averaged value per soil layer in SAP2000 in the H1 and H2 directions, and separate values per soil layer in the H1 and H2 directions in DEEPSOIL. The code-to-code verification of SAP2000 confirms its utility for equivalent-linear time-domain analysis of soil domains.

7.2 | Soil–Structure Interaction Analysis

To benchmark the ability of SAP2000 to capture the interaction between a (nuclear) structure and the supporting soil, a numerical representation of the Lotung experiment is developed in SAP2000, and its response is compared with recorded data. The Lotung experiment, which documented the response of a containment structure and a SG within, situated on a soft soil stratum in the seismically active region of Lotung, Taiwan, is widely recognized in the nuclear industry as a benchmark to validate finite element programs used for SSI analysis. Doulgerakis et al. [13] provide guidance for Commercial Grade Dedication (CGD) of software used for nonlinear seismic analysis, including SSI, of NPPs, and documents test cases to benchmark specific software features. Test Case 20 outlines a methodology to validate a finite element program for SSI analysis using the Lotung experiment data for a strong unidirectional earthquake recording. The modeling approach described in Doulgerakis et al. [13] is adopted in this study to verify SAP2000; see Section 3.3 of Lal et al. [3] for details.

Modal analysis of the fixed-base containment structure and SG, without the underlying soil, is performed to compare the resonant frequencies of the SAP2000 model with those reported in the CGD document. The frequencies matched well: 10.1 Hz (10.2 Hz) in SAP2000 versus 10.5 Hz (10.8 Hz) in the CGD document for the containment structure in the H1 (H2) direction, and 4.9 Hz (5.8 Hz) in SAP2000 versus 5.0 Hz (5.4 Hz) for the SG. Response-history analysis is performed using the FNA algorithm in SAP2000, and acceleration histories are extracted at five locations identified in the CGD document (1) near the boundary of the soil domain on the ground surface, representing surface free-field response, (2) the base of the containment structure, (3) the top of the containment structure, (4) the base of the SG, and (5) the top of the SG. Figure 6 enables a comparison of the numerically predicted and the experimentally recorded acceleration response spectra at the base and the top of the containment structure, with other results presented in Lal et al. [3].

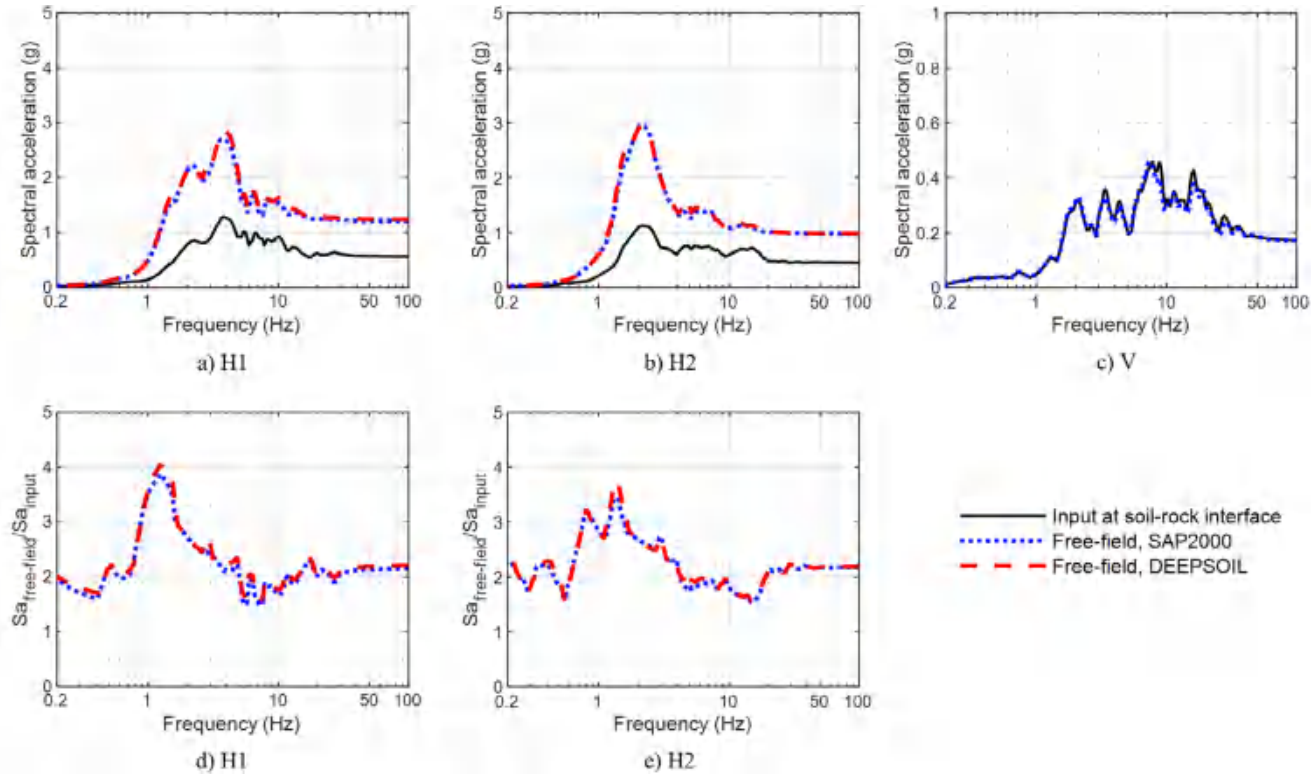

FIGURE 4 | Acceleration response spectra, 5% damping, soil profile S1, GM1C.

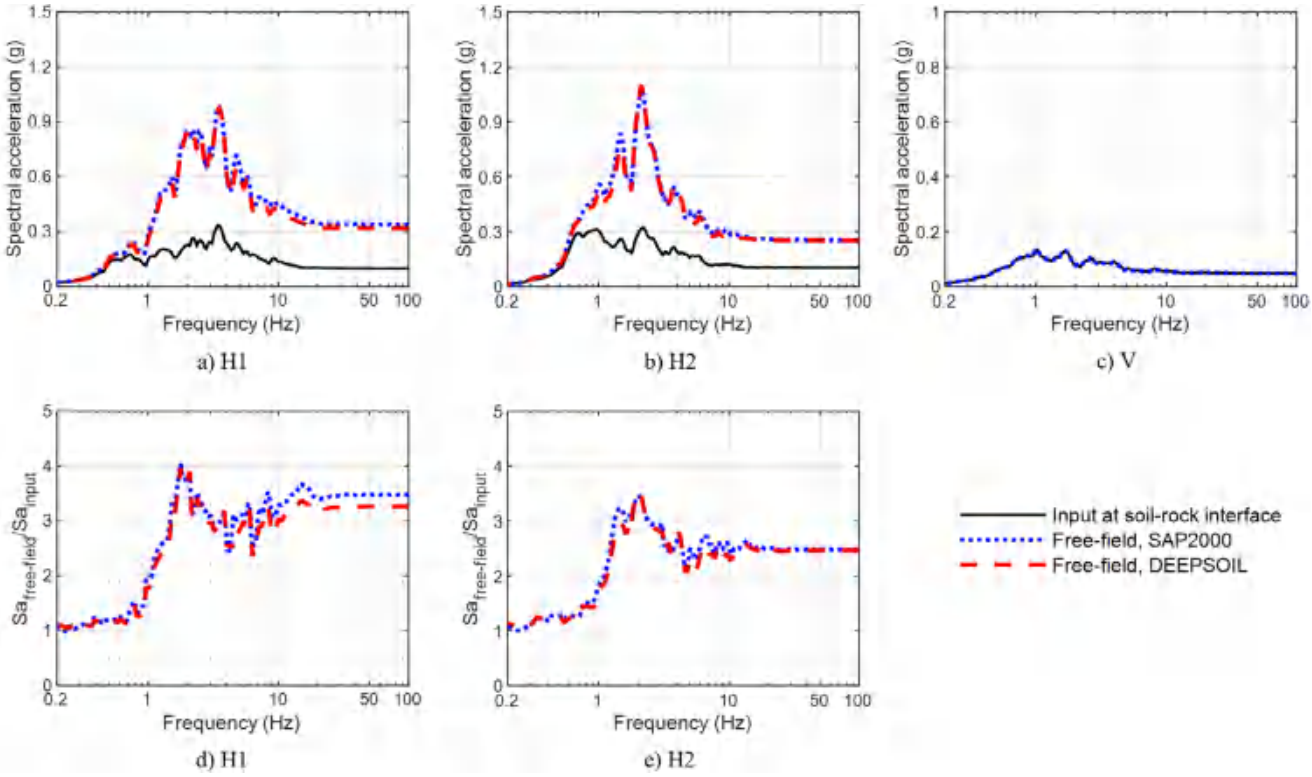

FIGURE 5 | Acceleration response spectra, 5% damping, soil profile S2, GM2A.

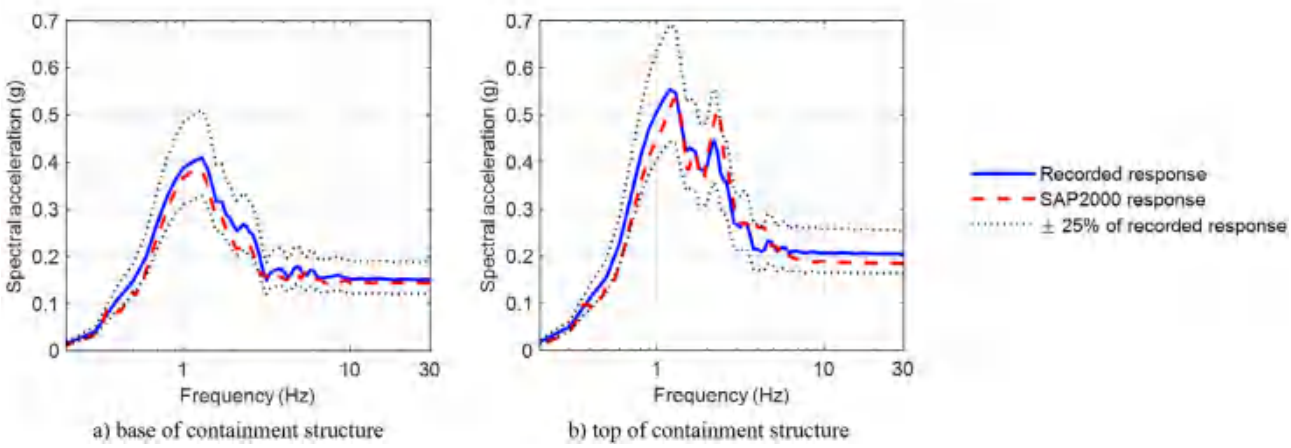

FIGURE 6 | Numerical and recorded responses of the Lotung experiment.

The CGD document outlines two acceptance criteria for validating a finite element program to capture SSI: (1) the numerical response should be within 25% of the recorded response, and (2) the shape of the acceleration spectra derived from the numerical and recorded responses should be similar. In Figure 6, the acceleration spectra from SAP2000 and the recorded data exhibit nearly identical shapes (i.e., similar frequencies for the dominant peaks), and the numerically predicted response is within 25% of the experimental data. Identical trends were observed at the other locations, validating the FNA algorithm to simulate SSI effects and predict in-structure response.

8 | Response-History Analysis

8.1 | Soil Domains

8.1.1 | Fundamental Site Frequencies

Table 1 presents the fundamental site frequencies for the seven APR1400 soil profiles considered in this study, determined by modal analysis in SAP2000. Values are reported for the low-strain (i.e., G_0) soil properties and for the degraded soil profiles with shear strains corresponding to the nine seismic inputs. A single value is reported for GM3 because it has both the horizontal components matched to the same broadband spectrum. As the intensity of shaking at the rock horizon is increased (e.g., GM1A to GM1C), the fundamental site frequency decreases, which is an expected outcome.

Soil profiles S1 and S2, which have the lowest shear wave velocities, and for which SSI effects, if any, would be maximized for all seven profiles considered, undergo a significant reduction in fundamental frequency for the high-intensity shaking (= 0.5 g geomean horizontal PGA): see the cells highlighted yellow in Table 1. This significant reduction is due to the large shear strains that develop in these profiles, resulting in a considerable decrease in their shear stiffness. The maximum shear strain in soil profile S1 (S2) for GM1C, GM2C, and GM3C is approximately 0.25% (0.65%), 1.9% (3%), and 0.3% (0.7%), respectively.

The use of equivalent-linear analysis and strain-compatible soil properties, to indirectly capture the soil nonlinearity in

TABLE 1 | Soil column fundamental frequencies (Hz)[a].

	S1		S2		S3		S4		S5		S6		S9	
	H1	H2	H1	H2	H1	H2	H1	H2	H1	H2	H1	H2	H1	H2
Low strain	1.5		1.9		2.3		2.9		3.7		5.6		12.5	
GM1A	1.4	1.4	1.7	1.7	2.3	2.2	2.8	2.8	3.6	3.6	5.4	5.4	11.7	11.7
GM1B	1.3	1.3	1.5	1.4	2.1	2.1	2.7	2.7	3.5	3.5	5.3	5.3	11.5	11.5
GM1C	1.2	1.2	1.3	1.2	2.0	2.0	2.5	2.6	3.5	3.5	5.2	5.3	11.4	11.4
GM2A	1.4	1.4	1.7	1.7	2.2	2.2	2.8	2.8	3.6	3.6	5.4	5.4	11.7	11.7
GM2B	1.1	1.1	1.3	1.3	2.1	2.0	2.7	2.7	3.5	3.5	5.3	5.3	11.5	11.5
GM2C	1.0	0.8	1.0	0.8	1.9	1.9	2.5	2.5	3.5	3.5	5.2	5.2	11.4	11.4
GM3A	1.4		1.7		2.2		2.8		3.6		5.4		11.7	
GM3B	1.2		1.4		2.1		2.7		3.5		5.3		11.5	
GM3C	1.1		1.1		2.0		2.6		3.5		5.2		11.4	

[a]Cells highlighted in yellow represent cases wherein the soil columns develop large shear strains and undergo a significant reduction in fundamental frequency.

site-response and SSI analysis, is considered valid for shear strains as high as 0.1% to 0.4% [29]. (For higher shear strains, nonlinear site-response and SSI analysis is recommended.) Although shear strains greater than 0.1% to 0.4% are predicted for the combinations of the two most flexible soil profiles and the most intense ground shaking, because (a) equivalent-linear analysis remains benchmark procedure for the United States nuclear industry, and (b) the objective here is to determine the importance of SSI analysis for base-isolated reactor buildings with a wide range of geometries, isolation systems, soil properties, and seismic inputs, and not to design a reactor building and its equipment, the consistent use of equivalent-linear analysis does not compromise either the outcomes or the recommendation of this study.

8.1.2 | Amplification of Seismic Inputs

The softer soil profiles S1, S2, S3, and S4 amplify the PGA by a factor of between 1.6 and 3.4, resulting in intense ground shaking at the surface free field for the high-intensity inputs: see, for example, panels (a) and (b) of Figure 4. The highest amplification of peak acceleration occurs for the lower intensity inputs, which is an expected outcome. For the stiffest soil column (S9), the peak accelerations at the horizon and the surface free field are approximately equal, namely, there is little-to-no amplification, which is another anticipated result.

8.2 | Reactor Buildings and Isolation Systems

8.2.1 | Overview

To determine the significance of SSI for base-isolated reactor buildings, responses for Case 1 (including SSI) and Case 3 (without SSI effects) of Figure 1 are compared in terms of:

1. Behavior of the isolation systems
   a. Horizontal force–displacement (FD) loops, that is, the plot of the total horizontal force in all the isolators versus the relative horizontal displacement of the basemat of a reactor building with respect to the bottom of the isolators.
   b. Peak resultant horizontal displacement, taken as the peak value of the resultant horizontal displacement computed at every time step.
2. Accelerations at two locations in each of the three isolated reactor buildings
   a. Peak resultant horizontal acceleration, taken as the peak value of the resultant horizontal acceleration computed at every time step.
   b. 5% damped acceleration response spectra in the horizontal and vertical directions. Acceleration histories from response-history analysis in SAP2000 are used to derive the acceleration response spectra. Acceleration histories are extracted in the isolated reactor buildings at the locations identified by the yellow solid circles in Figure 7.

For the sake of conciseness, a limited number of response-history analysis results are presented in this study. Readers interested in the complete dataset are directed to Lal et al. [3] and its companion digital appendix.

8.2.2 | Viable Isolation Systems

Two metrics for selecting a site-specific isolation system are (1) ratio of isolation-system frequency to the fundamental frequency of the superstructure and the fundamental frequency of the supporting soil domain, and (2) isolator displacement capacity. Separating the fundamental frequencies of a non-isolated superstructure from its supporting soil domain has been good structural engineering practice for decades, avoiding possible resonance in the superstructure, and large acceleration responses for small-amplitude inputs. Similarly, for isolated buildings, superstructures are designed to be much stiffer than the isolation system to maximize the benefits of isolation, driving nearly all the displacement demand into the isolators, and minimizing drift in the superstructure.

The horizontal displacement capacities of the five isolation systems, sized for the three reactor buildings using the procedures of Constantinou et al. [22], are (a) 1-second system: 50 mm to 100 mm, (b) 2-second system: 250 mm to 350 mm, and (c) 3-second system: 500 mm to 700 mm, with the range dependent on the number of isolators used. Peak horizontal displacement greater than these capacities will likely require the use of an alternate isolation system, regardless of whether SSI is modeled (Case 1) or not (Case 3). (An alternate isolation system could include the addition of damping or the use of a longer period system, such as B3 replacing L2A.)

In the next section, attention is focused on those isolation systems that are considered viable, assumed hereafter to require that (1) the period of the isolation system to be equal to or greater than 110% of the period of the degraded soil column (i.e., if the period of the degraded soil column is 1 second, the period of the isolation system can be no less than 1.1 seconds), and (2) horizontal displacement to be equal to or less than 125% of the upper bound on the ranges given above, namely, 125 mm for a 1-second isolation system (L1), 425 mm for a 2-second isolation system (L2A, L2B, and B2), and 875 mm for a 3-second isolation system (B3). This results in 826 analysis combinations (out of 945 analyzed) with viable isolation systems. (In practice, non-viable isolation systems would not be pursued.)

8.2.3 | Results

8.2.3.1 | Isolation Systems. The soil domain beneath a base-isolated building may affect the behavior of the isolation system by increasing the overall system flexibility and introducing additional energy dissipation through damping in the soil, which is investigated here. Table 2 presents the peak resultant horizontal isolation system displacements for the FHR building and three of the softest soil profiles S1, S2, and S3 (for which SSI effects, if any, will be maximized), along with the percentage difference between the values for Cases 1 and 3. (Similar tables are presented in Lal et al. [3] for the other two reactor buildings and four soil profiles.) In this table, a positive percentage difference indicates that the displacements calculated using the surface free-field inputs (Case 3) are greater than those calculated by analysis of a coupled soil-structure model (Case 1). A negative percentage difference indicates that the Case 1 displacements are

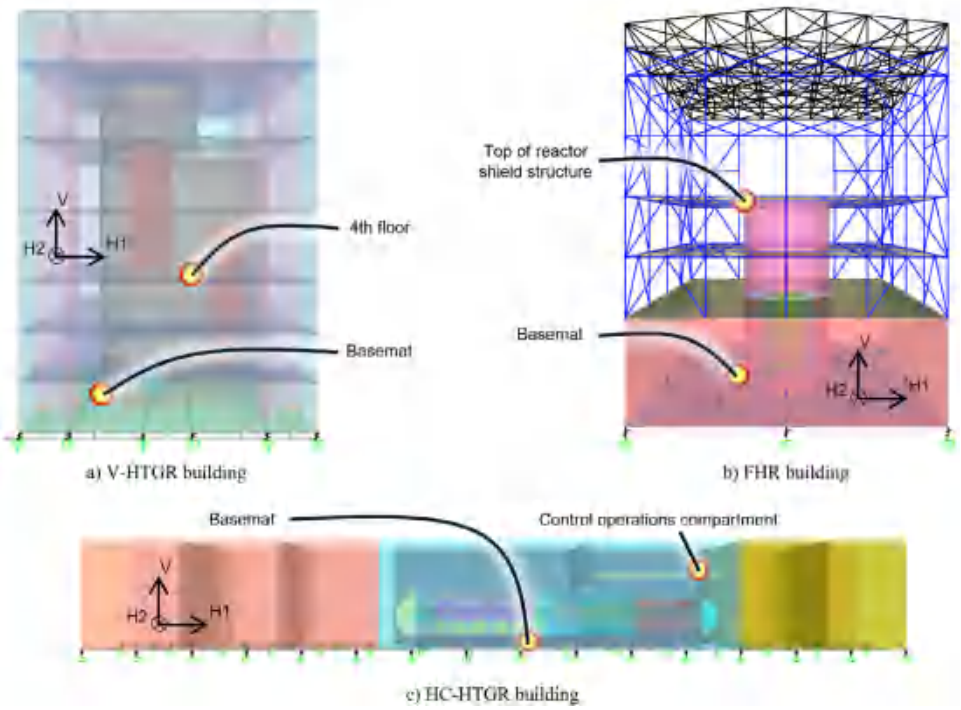

FIGURE 7 | Locations for monitoring acceleration responses.

greater. The shaded cells are associated with non-viable isolation systems associated with either excessive displacement (purple) or both excessive displacement and nearly identical isolation system and degraded soil column periods (red). Although data is presented for non-viable isolation systems for completeness and transparency, the outcomes and conclusions below are based solely on results for the viable isolation systems. Panels (g) and (h) of Figures 8 through 10 present the horizontal FD loops for three combinations with viable isolation systems and the softest soil profile S1. (Results for all analysis cases can be found in Lal et al. [3] and its digital appendix.)

In Table 2, the peak resultant horizontal displacements for Case 3 are generally greater than or equal to those for Case 1 in most combinations with viable isolation systems but are no more than 4% smaller than those for Case 1. Similarly, the FD loops in Figures 8 through 10 for Cases 1 and 3 are virtually the same. Identical trends were observed for the peak resultant horizontal displacements and FD loops for the viable isolation systems not presented here. Across all reactor buildings, soil domains, seismic inputs, and viable isolation systems, the mean of the ratio of peak resultant horizontal displacements for Case 3 to Case 1 is 1.01 with a coefficient of variation (COV) or 0.03. The mean (COV) of the ratio for the five isolation systems is 1.01 (0.04) [L1], 1.01 (0.02) [L2A], 1.00 (0.02) [L2B], 1.00 (0.03) [B2], and 1.01 (0.02) [B3]. The isolation-system responses are virtually identical for Cases 1 and 3.

8.2.3.2 | Reactor Buildings. Table 3 presents the peak resultant horizontal accelerations for the FHR building supported on soil profile S1. The percentage difference between the values of Case 1 and Case 3 is also presented, with a negative difference identifying higher accelerations if SSI analysis is performed. The focus here is horizontal acceleration because only 2D isolation systems are considered in this study. For transparency, data from all combinations are presented, but those associated with non-viable isolation systems per Table 2 are highlighted in yellow. Identical to the discussion on isolation-system responses, outcomes, and conclusions are derived solely from the analysis results of combinations with viable isolation systems.

Figures 8 through 10 present the acceleration response spectra for soil profile S1 for (1) the V-HTGR building, isolation system L1, and seismic input GM3A; (2) the HC-HTGR building, isolation system L2B, and seismic input GM2B; and (3) the FHR building, isolation system B3, and seismic input GM1C. In-structure acceleration response spectra provide inputs for the design and qualification of safety-class equipment. Herein, the frequency range of interest is chosen to be 2 Hz to 50 Hz, which brackets, with margin, the fundamental frequencies of the safety-class equipment in the three reactor buildings. The range of 2 Hz to 50 Hz is emphasized in the figures, with spectral responses outside the bounds shaded in gray.

In Table 3, the Case 3 peak resultant horizontal accelerations either exceed those for Case 1 or are at most 15% less: GM1C, L2B. Although 15% might appear to be appreciable, the difference between the Case 1 and Case 3 results of 0.03 g is insignificant from an engineering perspective. The horizontal acceleration response spectra at the two monitoring locations in each reactor building, as presented in Figures 8 through 10, are functionally identical for Cases 1 and 3. Identical outcomes were observed for all other combinations of reactor building, soil profile, seismic input, and viable isolation systems, as presented in the digital appendix to Lal et al. [3]. The ratio of Case 3 to Case 1 peak resultant horizontal accelerations, for all reactor buildings, soil domains, seismic inputs, and viable isolation systems, has

TABLE 2 | Peak resultant horizontal isolation system displacements, FHR building (mm).

		L1			L2A			L2B			B2			B3		
	GM	Case 1	Case 3	%	Case 1	Case 3	%	Case 1	Case 3	%	Case 1	Case 3	%	Case 1	Case 3	%
Soil profile S1	GM1A	23	24	4	34	34	0	25	25	0	35	35	0	32	33	3
	GM1B	67	69	3	93	95	2	68	69	1	83	82	−1	85	86	1
	GM1C	106	112	6	142	147	4	102	105	3	118	115	−3	122	123	1
	GM2A	81	80	−1	189	192	2	112	113	1	99	99	0	97	98	1
	GM2B	356	312	−12	570	586	3	397	396	0	500	505	1	382	384	1
	GM2C	640	535	−16	1344	1350	0	833	834	0	1262	1230	−3	925	906	−2
	GM3A	59	59	0	115	115	0	78	78	0	85	84	−1	94	95	1
	GM3B	190	183	−4	360	369	3	249	251	1	266	271	2	312	312	0
	GM3C	336	318	−5	639	652	2	458	454	−1	590	600	2	587	574	−2
Soil profile S2	GM1A	24	25	4	28	28	0	22	23	5	34	36	6	32	33	3
	GM1B	66	68	3	80	82	3	61	62	2	85	85	0	78	79	1
	GM1C	94	103	10	113	121	7	84	88	5	115	111	−3	113	113	0
	GM2A	62	61	−2	166	170	2	96	97	1	77	77	0	76	78	3
	GM2B	269	245	−9	476	484	2	314	310	−1	360	362	1	303	291	−4
	GM2C	579	421	−27	1163	1193	3	717	679	−5	1039	1000	−4	790	775	−2
	GM3A	51	52	2	99	101	2	67	68	1	70	70	0	86	88	2
	GM3B	177	173	−2	315	314	0	207	211	2	203	210	3	283	283	0
	GM3C	296	267	−10	525	520	−1	358	365	2	422	445	5	486	481	−1
Soil profile S3	GM1A	15	15	0	18	18	0	13	13	0	22	22	0	20	20	0
	GM1B	45	46	2	51	51	0	39	40	3	64	63	−2	52	52	0
	GM1C	77	78	1	89	88	−1	70	70	0	92	92	0	83	82	−1
	GM2A	48	47	−2	155	155	0	87	86	−1	51	51	0	90	90	0
	GM2B	137	139	1	450	449	0	249	248	0	269	275	2	276	278	1
	GM2C	228	227	0	730	732	0	407	408	0	538	550	2	446	458	3
	GM3A	32	32	0	92	91	−1	58	57	−2	47	47	0	67	66	−1
	GM3B	96	97	1	267	264	−1	169	167	−1	129	128	−1	228	225	−1
	GM3C	160	163	2	434	431	−1	277	275	−1	310	309	0	391	386	−1

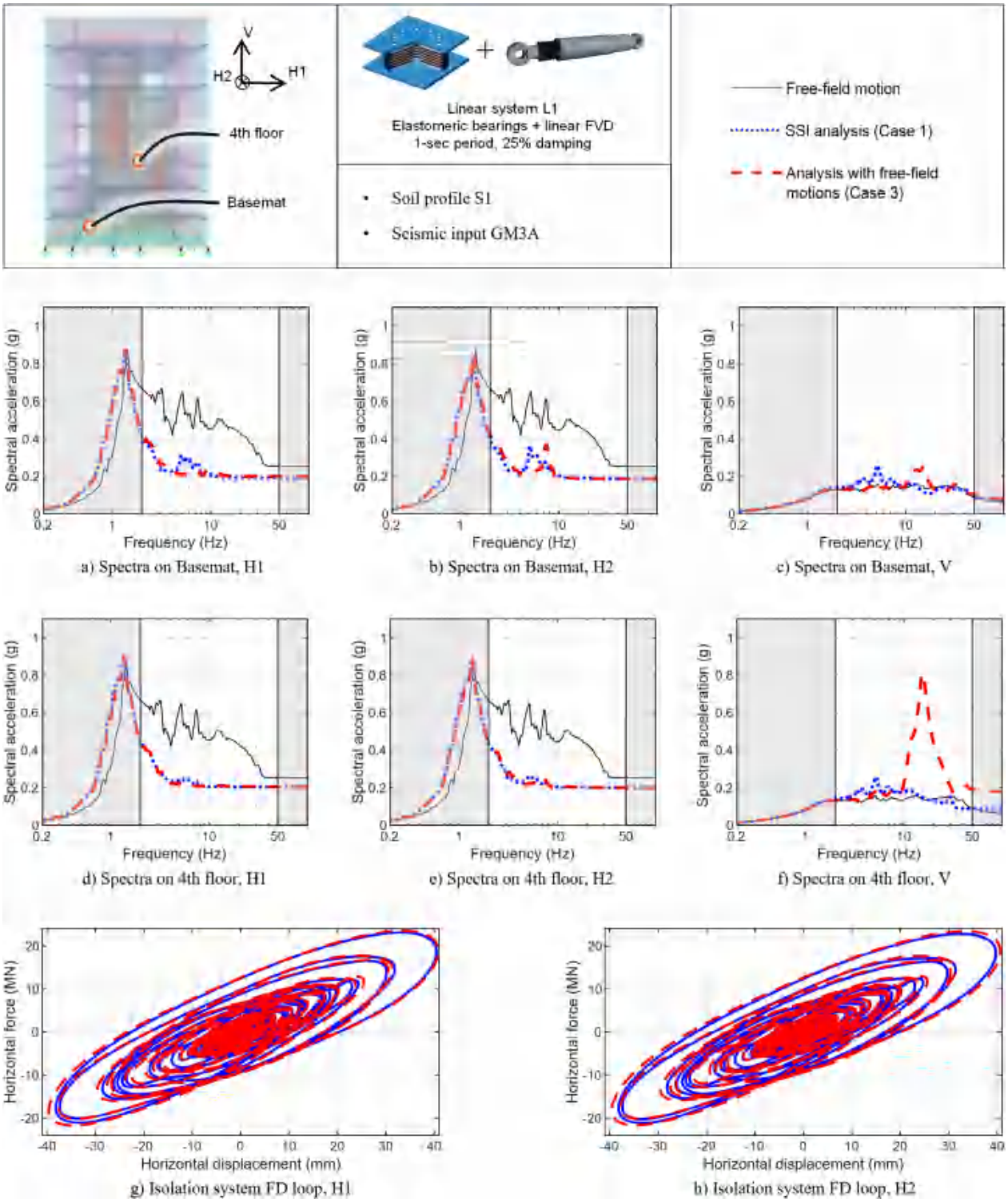

FIGURE 8 | Acceleration response spectra, 5% damping, and isolation system FD response,V-HTGR building, isolation system L1, soil profile S1, seismic input GM3A.

a mean and COV of 0.99 and 0.06, respectively. For the five isolation systems, the mean (COV) of the ratio of peak horizontal accelerations is 0.99 (0.06) [L1], 1.01 (0.08) [L2A], 0.99 (0.07) [L2B], 0.99 (0.05) [B2], and 1.00 (0.06) [B3].

In the vertical direction, the spectral peaks for Case 3 correspond to the fundamental vertical frequencies of the isolated reactor buildings, whereas those for Case 1 align with the fundamental frequencies of the soil-isolator-structure systems (listed in Table 4-3 in Lal et al. [3]). With respect to Case 3, the Case 1 spectral peaks are (1) at lower frequencies because of the added vertical flexibility of the soil domains (e.g., see panels (c) and (f) of Figure 8 wherein the dominant peaks are at 16 Hz for Case 3 and 5 Hz for Case 1), and (2) generally smaller in amplitude

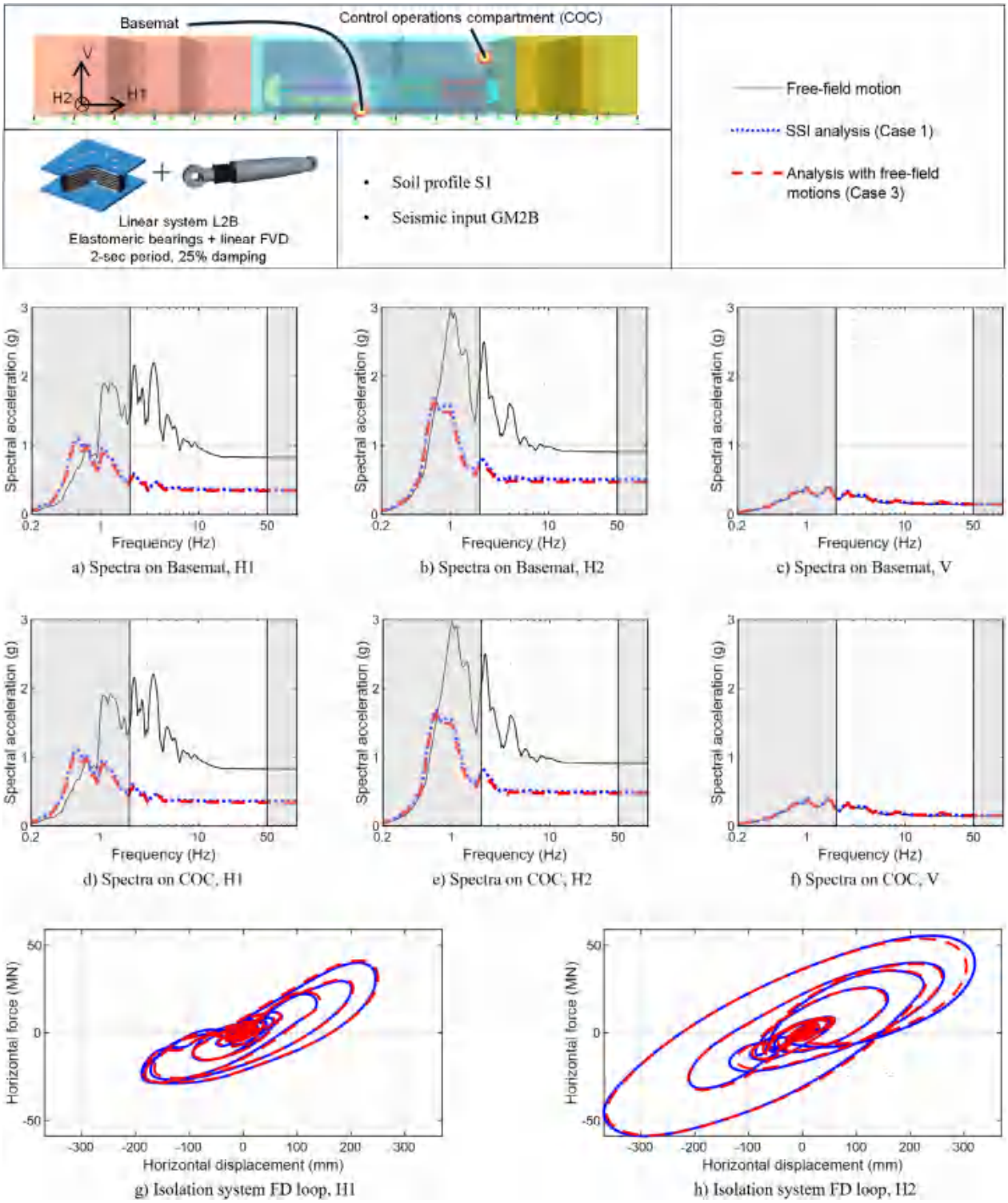

FIGURE 9 | Acceleration response spectra, 5% damping, and isolation system FD response, HC-HTGR building, isolation system L2B, soil profile S1, and seismic input GM2B.

due to the added damping of the soil domain, namely, SSI in the vertical direction reduces seismic demands[9]. Similar observations were made by Drosos and Sitar [7] and Zhou and Wei [10] regarding vertical response from the SSI analyses of a base-isolated APR1400 building. (Herein, for the HC-HTGR building response in Figure 9, there is little-to-no amplification of vertical spectral accelerations along its height since it is nearly rigid in the vertical direction.)

9 | Summary and Conclusions

The effects of SSI must be addressed for the design of NPPs in the United States. The current rules and guidance for SSI analysis assume that reactor buildings are both massive and stiff, which are the two key ingredients for significant SSI on soil sites. Seismic isolation can mitigate the impact of the seismic load case by adding 2D or 3D flexibility at the base of a reactor building,

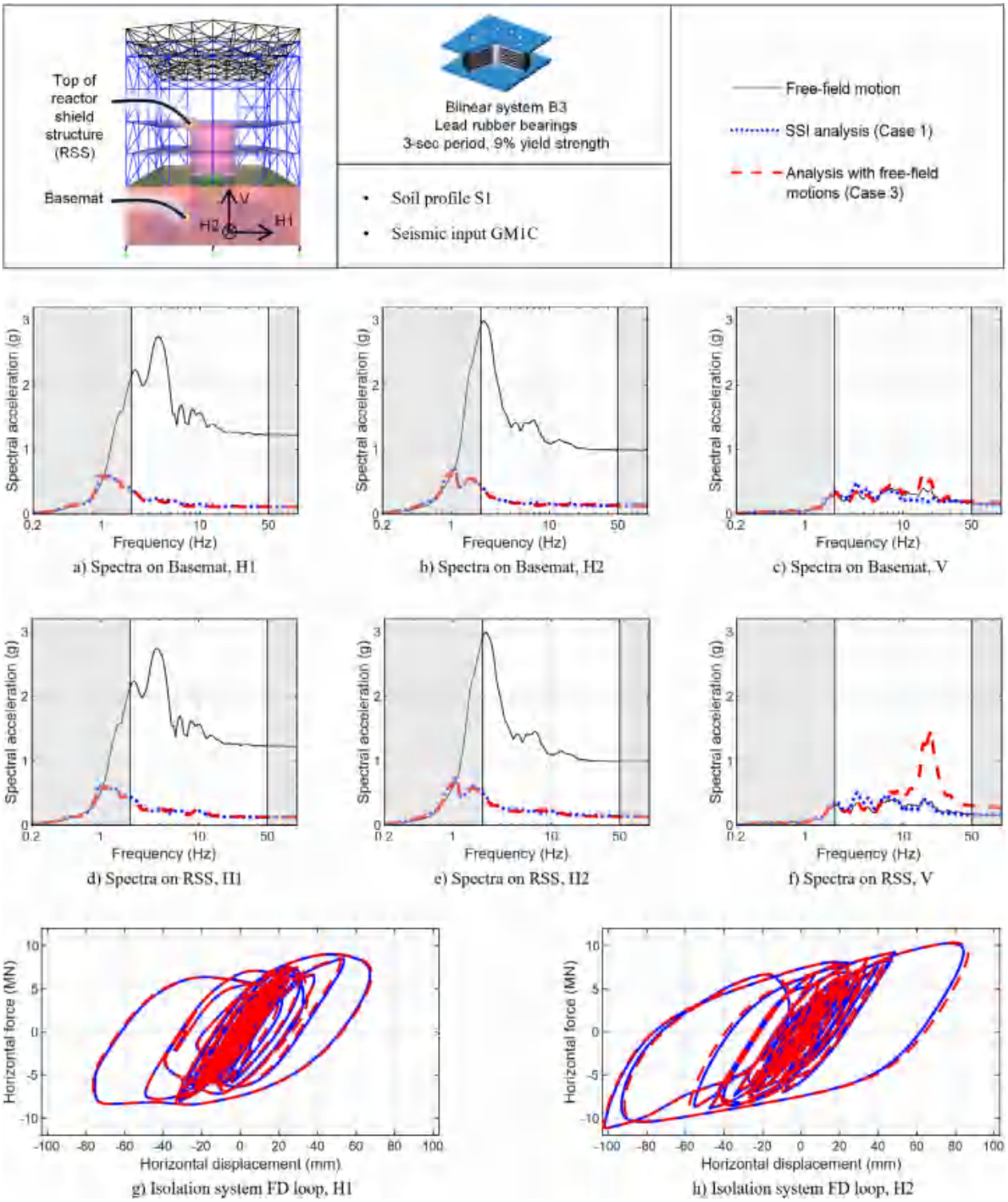

FIGURE 10 | Acceleration response spectra, 5% damping, and isolation system FD response, FHR building, isolation system B3, soil profile S1, seismic input GM1C.

removing a key component for significant SSI, leading to the hypothesis that SSI effects may be negligible for such buildings. Determining whether this hypothesis is correct is the focus of this study, which addresses three fundamentally different reactor buildings, five horizontal isolation systems incorporating isolators and dampers available in the United States at this time, seven soil profiles extracted from the DCDs of the APR1400 pressurized water reactor, and nine seismic inputs collectively covering a very broad range of frequencies and intensities of shaking.

To investigate the influence of SSI on base-isolated reactor buildings, response-history analysis was performed for three cases: (1) analysis of the coupled soil-structure systems to include the effects of SSI, if any, (2) site-response analysis using the

TABLE 3 | Peak resultant horizontal accelerations, FHR building, soil profile S1 (g).

		L1			L2A			L2B			B2			B3		
	Location	**Case 1**	**Case 3**	**%**	**Case 1**	**Case 3**	**%**	**Case 1**	**Case 3**	**%**	**Case 1**	**Case 3**	**%**	**Case 1**	**Case 3**	**%**
GM1A	Free field	0.31	0.31	0	0.31	0.31	0	0.31	0.31	0	0.31	0.31	0	0.31	0.31	0
	Basemat	0.12	0.12	0	0.04	0.04	0	0.04	0.04	0	0.16	0.16	0	0.09	0.09	0
	RSS	0.13	0.13	0	0.04	0.04	0	0.04	0.04	0	0.17	0.17	0	0.1	0.1	0
GM1B	Free field	0.81	0.81	0	0.81	0.81	0	0.81	0.81	0	0.81	0.81	0	0.81	0.81	0
	Basemat	0.36	0.34	−6	0.1	0.1	0	0.1	0.1	0	0.22	0.22	0	0.12	0.12	0
	RSS	0.39	0.37	−5	0.11	0.1	−9	0.12	0.11	−8	0.24	0.24	0	0.14	0.13	−7
GM1C	Free field	1.24	1.24	0	1.24	1.24	0	1.24	1.24	0	1.24	1.24	0	1.24	1.24	0
	Basemat	0.58	0.55	−5	0.15	0.15	0	0.17	0.16	−6	0.25	0.25	0	0.14	0.14	0
	RSS	0.66	0.59	−11	0.16	0.16	0	0.2	0.17	−15	0.29	0.27	−7	0.16	0.15	−6
GM2A	Free field	0.35	0.35	0	0.35	0.35	0	0.35	0.35	0	0.35	0.35	0	0.35	0.35	0
	Basemat	0.39	0.38	−3	0.19	0.19	0	0.14	0.14	0	0.24	0.24	0	0.13	0.13	0
	RSS	0.42	0.39	−7	0.2	0.2	0	0.14	0.14	0	0.24	0.24	0	0.13	0.13	0
GM2B	Free field	0.93	0.93	0	0.93	0.93	0	0.93	0.93	0	0.93	0.93	0	0.93	0.93	0
	Basemat	1.76	1.44	−18	0.6	0.59	−2	0.53	0.49	−8	0.62	0.61	−2	0.25	0.24	−4
	RSS	1.85	1.49	−19	0.6	0.6	0	0.54	0.5	−7	0.61	0.62	2	0.25	0.25	0
GM2C	Free field	1.36	1.36	0	1.36	1.36	0	1.36	1.36	0	1.36	1.36	0	1.36	1.36	0
	Basemat	2.82	2.34	−17	1.48	1.37	−7	1.27	1.01	−20	1.38	1.24	−10	0.5	0.48	−4
	RSS	3.01	2.38	−21	1.48	1.38	−7	1.26	1.02	−19	1.41	1.25	−11	0.5	0.48	−4
GM3A	Free field	0.36	0.36	0	0.36	0.36	0	0.36	0.36	0	0.36	0.36	0	0.36	0.36	0
	Basemat	0.3	0.29	−3	0.12	0.12	0	0.1	0.1	0	0.23	0.23	0	0.13	0.13	0
	RSS	0.32	0.31	−3	0.12	0.12	0	0.11	0.11	0	0.24	0.23	−4	0.13	0.13	0
GM3B	Free field	0.89	0.89	0	0.89	0.89	0	0.89	0.89	0	0.89	0.89	0	0.89	0.89	0
	Basemat	1.03	0.86	−17	0.38	0.37	−3	0.33	0.31	−6	0.41	0.4	−2	0.23	0.23	0
	RSS	1.07	0.92	−14	0.39	0.38	−3	0.35	0.32	−9	0.42	0.41	−2	0.23	0.23	0
GM3C	Free field	1.36	1.36	0	1.36	1.36	−1	1.36	1.36	0	1.36	1.36	0	1.36	1.36	0
	Basemat	1.68	1.44	−14	0.68	0.66	−3	0.61	0.56	−8	0.73	0.71	−3	0.35	0.34	−3
	RSS	1.77	1.49	−16	0.69	0.67	−3	0.64	0.58	−9	0.75	0.72	−4	0.35	0.34	£3

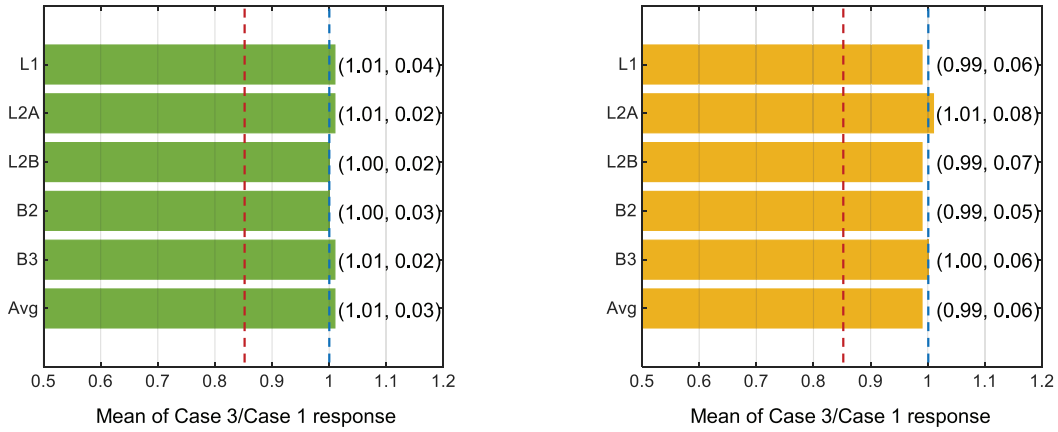

a) isolation system horizontal displacements

b) in-structure horizontal acceleration

FIGURE 11 | Ratios of peak responses for Case 3 (no SSI) to Case 1 (including SSI).

same soil domains and seismic inputs from Case 1 to determine surface free-field motions, capturing the amplification or de-amplification of ground motions from the base of a soil profile to the ground surface in the absence of a structure, and (3) analysis of the seismically isolated reactor buildings using the surface free-field motions from Case 2, without the supporting soil domains, that is, ignoring SSI.

The influence of SSI was evaluated by comparing the responses of Cases 1 and 3. If the Case 1 responses are *similar* to or less than those in Case 3, SSI is either of little engineering importance or advantageous. Given the list of assumptions that must be made for SSI analysis, namely, simplifying a soil domain into a number of horizontal layers, assigning properties to each of the layers, identifying a horizontal (rock) horizon at depth, characterizing ground motion at the horizon for input at the base of soil domains, assuming vertical propagation of body waves from the rock horizon to the surface of soil domains (i.e., ignoring surface waves and inclined body waves), and idealizing the boundaries of soil domain, responses were deemed *similar* if they were within 15%.

Figure 11 summarizes the key results of this study by presenting the Case 3 to Case 1 ratios of peak resultant horizontal isolation-system displacement (Figure 11a) and peak resultant horizontal in-structure acceleration[10] (Figure 11b). Data are organized by isolator type (L1, L2A, L2B, B2, and B3) for all 826 viable isolation solutions (of the 945 analyzed). The mean of the ratios and the corresponding COV are presented in parentheses: (mean, COV). Values averaged across all five isolation systems are also presented in the last row of the figures (i.e., Avg). The vertical dashed blue lines in the figures identify a mean of 1.0. The vertical red dashed lines identify a mean of 0.85, for which the Case 3 predictions would systematically underestimate the Case 1 predictions. The outcomes do not challenge the 15% threshold identified above.

The results presented in Section 8.2.3 and summarized above make clear that SSI has no meaningful effect on the response of surface- or near-surface-founded, horizontally isolated reactor buildings, including forces and displacements in the isolation system and in-structure horizontal accelerations[11]. In-structure spectra for design and qualification of safety-related equipment and peak horizontal displacements for the design of isolators and dampers can be established using surface-free-field representations of ground shaking. These recommendations apply to all NPPs, regardless of size, from GW-scale LLWRs to MW-scale microreactors.

Acknowledgments

The information, data, or work presented herein was funded by the United States Department of Energy under its Advanced Reactor Concept (ARC-20) project, Award Number DE-NE0009049. The views and opinions of the authors expressed herein do not necessarily state or reflect those of the United States Government or any agency thereof, University at Buffalo, Massachusetts Institute of Technology, Applied Geodynamics, Simpson Gumpertz & Heger, and Structural Integrity Associates. The authors thank Professor Youssef Hashash at the University of Illinois at Urbana-Champaign for his support with our use of DEEPSOIL. The authors also thank Professors Michael Constantinou and Mettupalayam Sivaselvan, and Dr. Sai Sharath Parsi at the University at Buffalo, and Ms. Natalie Doulgerakis at Structural Integrity Associates for their valuable contributions to the study.

Conflicts of Interest

The authors declare no conflicts of interest.

Data Availability Statement

The data that support the findings of this study are available from the corresponding author upon reasonable request.

Endnotes

[1] Base isolation is likely not an economical solution for deeply embedded reactor buildings because (a) much additional excavation will be needed to accommodate the lateral displacement of the isolated superstructure, and (b) the perimeter retaining wall will be expensive to construct and monitor for the lifetime of the plant.

[2] The stiffness of the soil springs is calculated per tables and a figure presented in the ASCE/SEI 4-16, developed by Whitman and Richart [30]. The half-space assumed in the development of the spring constants is assigned a single value of shear modulus, assumed to be low strain, and Poisson's ratio. This representation of a foundation medium is simple, as required for an analytical solution.

[3]The alternative to FNA in SAP2000 for time-domain analysis is *direct integration*, which is computationally more expensive.

[4]These bilinear systems could also have been characterized by single or triple concave spherical sliding bearings with a similar force–displacement hysteresis. Information on spherical sliding bearings can be found in Constantinou et al. [22].

[5]The peak ground shaking required to activate a bilinear isolation system can be taken as one third of the *yield strength* of the isolation system, namely, PGA = 0.05 g for system B2 and PGA = 0.03 g for system B3, both of which are insignificant.

[6]The user-specified shear modulus degradation and damping curves input to DEEPSOIL are taken from the APR1400 Design Certification Documents.

[7]There is no industry consensus on vertical site-response analysis. An alternative process to generate vertical inputs at the base of the soil domain was considered for the study but was set aside because it was cumbersome, not central to the analysis presented in the paper, and technically no more justified than the adopted method. The alternative process for each combination of soil profile (7), ground motion triplet (3), and intensity (3), involved the following steps: (a) generate a horizontal surface-free-field spectrum by site-response analysis, (b) select a frequency-dependent V/H relationship from those available in the literature, (c) using (a) and (b) develop a vertical surface-free-field spectrum, (d) generate an acceleration time series consistent with the vertical spectrum of (c), and (e) deconvolve the time series of (d) to the base of the soil profile.

[8]See Appendix C of Lal et al. [3] for information on *within* and *outcrop* motions, and their application at the base of a soil profile.

[9]See Figure 8f: the peak vertical spectral demand is 0.8 g for Case 3 and 0.22 g for Case 1. If a relatively larger spectral acceleration is problematic for supported equipment, SSI analysis in the vertical direction might be justified. Alternately, damping in the vertical direction can be augmented with an appropriate value corresponding to that of the supporting soil domain to indirectly account for the added soil damping.

[10]Computed as the maximum of the square root of the sum of squares (SRSSs) of the acceleration histories in the two horizontal directions.

[11]This outcome is not inconsistent with (1) Section 5.1.1 of ASCE/SEI Standard 4-16 (see Section 3 of this paper), namely, a flexible structure (enabled here by base isolation) constructed on a (relatively) stiff soil domain, can be analyzed assuming a fixed base, without explicit modeling of the soil domain, and (2) Constantinou and Kneifati [4–6] who, more than 30 years ago, established that SSI effects on base-isolated structures were less significant than those for conventionally founded (or non-isolated) structures, with little-to-no effect in many cases.

References

1. S. S. Parsi, K. M. Lal, B. D. Kosbab, E. D. Ingersoll, K. Shirvan, and A. S. Whittaker, "Seismic Isolation: A Pathway to Standardized Advanced Nuclear Reactors," *Nuclear Engineering and Design* 387 (2022): 111445, https://doi.org/10.1016/j.nucengdes.2021.111445.

2. C. Bolisetti and A. S. Whittaker, "Site Response, Soil-Structure Interaction and Structure-Soil-Structure Interaction for Performance Assessment of Buildings and Nuclear Structures," in *Technical Report MCEER-15-0002* (University at Buffalo, State University of New York, 2015).

3. K. M. Lal, A. S. Whittaker, B. D. Kosbab, S. Vahdani, K. Shirvan, and S. S. Parsi, "Considerations of Soil-Structure-Interaction for Seismically Isolated Nuclear Reactor Buildings," in *Technical Report MCEER-24-0003* (University at Buffalo, State University of New York, 2024).

4. M. C. Constantinou and M. C. Kneifati, "Dynamics of Soil-Base-Isolated-Structure Systems, Report 1: Linear Systems," in *Report to the U.S. National Science Foundation* (Drexel University, 1986).

5. M. C. Constantinou and M. C. Kneifati, "Dynamics of Soil-Base-Isolated-Structure Systems," *Journal of Structural Engineering* 114, no. 1 (1988): 211–221.

6. M. C. Constantinou and M. C. Kneifati, "Dynamics of Soil-Base-Isolated-Structure Systems, Report 3: Nonlinear Systems," in *Report to the U.S. National Science Foundation* (Drexel University, 1986).

7. V. A. Drosos and N. Sitar, "Soil-Structure Interaction Effects on Seismically Isolated Nuclear Power Plants." in *Proceedings: International Foundations Congress and Equipment Expo 2015*, San Antonio, TX (2015).

8. United States Nuclear Regulatory Commission (USNRC), "Design Response Spectra for Seismic Design of Nuclear Power Plants," in *Regulatory Guide 1.60* (1973).

9. F. Ostadan and N. Deng, *Computer Program SASSI 2010 V1.0: A System for Analysis of Soil-Structure Interaction* (Geotechnical and Hydraulic Engineering Services, Bechtel National Inc., 2012).

10. Z. Zhou and X. Wei, "Seismic Soil-Structure Interaction Analysis of Isolated Nuclear Power Plants in Frequency Domain," *Shock and Vibration* 2016, no. 1 (2016): 1–15.

11. American Society of Civil Engineers (ASCE), "Seismic Analysis of Safety-Related Nuclear Structures and Commentary." in *ASCE/SEI 4-16* (2017).

12. United States Nuclear Regulatory Commission (USNRC), "Standard Review Plan for Seismic System analysis," in *NUREG-0800, Section 3.7.2* (2013).

13. N. Doulgerakis, P. K. Tehrani, I. Talebinejad, B. D. Kosbab, M. Cohen, and A. S. Whittaker, "Software Verification and Validation Guidance for Nonlinear Seismic analysis," in *Report Developed under DOE Grant Number DE-NE0008857* (United States Department of Energy, 2021), https://doi.org/10.2172/1831343.

14. Dassault Systèmes (Dassault), *Computer Program ABAQUS/CAE* (2024).

15. Livermore Software Technology Corporation (LSTC), *Computer Program LS-DYNA (Version R 14.0)* (2023).

16. Computers and Structures Incorporated (CSI), Computer Program SAP2000 (Version 25.0.0) (2023).

17. S. S. Parsi, K. M. Lal, E. Velez, et al., "Seismic Engineering of a Horizontal, Compact High Temperature Gas Reactor," in *Proceedings: International Congress on Advances in Nuclear Power Plants (ICAPP-24)*, Las Vegas, NV (2024).

18. F. U. H. Mir, C.-C. Yu, B. M. Carmichael, et al., "Guidelines for Implementing Seismic Base Isolation in Advanced Nuclear Reactors," in *Technical Report MCEER-24-0001* (University at Buffalo, State University of New York, 2024).

19. M. Kumar, A. S. Whittaker, and M. C. Constantinou, "Seismic Isolation of Nuclear Power Plants Using Elastomeric bearings," in *NUREG/CR-7255* (United States Nuclear Regulatory Commision, 2019), ML19063A541.

20. N. Makris and M. C. Constantinou, "Viscous Dampers: Testing, Modeling, and Application in Vibration and Seismic Isolation," in *Technical Report NCEER-90-0028* (University at Buffalo, State University of New York, 1990).

21. J. M. Kelly, M. S. Skinner, and K. E. Beucke, "Experimental Testing of an Energy-Absorbing Base Isolation System," in *UCB/EERC-81/17* (Earthquake Engineering Research Center, University of California, 1980).

22. M. C. Constantinou, A. S. Whittaker, Y. Kalpakidis, D. M. Fenz, and G. P. Warn, "Performance of Seismic Isolation Hardware under Service and Seismic Loading," in *Technical Report MCEER-07-0012* (University at Buffalo, State University of New York, 2007).

23. American Society of Civil Engineers (ASCE), "Minimum Design Loads for Buildings and Other Structures," in *ASCE/SEI 7-22* (2021).

24. F. U. H. Mir, K. M. Lal, B. D. Kosbab, et al., "Earthquake-Simulator Experiments of a Model of a Seismically-Isolated, Fluoride-Salt Cooled High-Temperature Reactor," in *Technical Report MCEER-22-0004* (University at Buffalo, State University of New York, 2022).

25. J. Hancock, J. Watson-Lamprey, N. A. Abrahamson, et al., "An Improved Method of Matching Response Spectra of Recorded Earthquake Ground Motion Using Wavelets," *Journal of Earthquake Engineering* 10, no. spec01 (2006): 67–89.

26. A. A. Sarlis and M. C. Constantinou, "Modelling Triple Friction Pendulum Isolators in Program SAP2000," in *Supplement to Technical Report MCEER 05-0009* (University at Buffalo, State University of New York, 2010), https://figshare.com/articles/presentation/Modeling_triple_friction_pendulum_isolators_in_program_SAP2000/25139669.

27. Y. M. A. Hashash, M. I. Musgrove, J. A. Harmon, et al., *DEEPSOIL 7.0, User Manual* (University of Illinois at Urbana-Champaign, 2020).

28. J. Lysmer and R. L. Kuhlemeyer, "Finite Dynamic Model for Infinite Media," *Journal of the Engineering Mechanics Division* 95, no. 4 (1969): 859–877.

29. B. Kim, Y. M. Hashash, J. P. Stewart, et al., "Relative Differences Between Nonlinear and Equivalent-Linear 1-D Site Response Analyses," *Earthquake Spectra* 32, no. 3 (2016): 1845–1865.

30. R. V. Whitman and F. Richart Jr, "Design Procedures for Dynamically Loaded Foundations," *Journal of the Soil Mechanics and Foundations Division* 93, no. 6 (1967): 169–193.